RSC Advances

ROYAL SOCIETY
OF CHEMISTRY

www.rsc.org/advances

Synergistic Effects of BHDB-IPC with AlPi/MCA on Flame Retarding TPEE

Luchong Zhang, Wei Wu*, Yuhua Zhong, Songwei Zhu, Zheng Wang, Zhiqiang Zou

Sino-German Joint Research Center of Advanced Materials，School of Materials Science and Engineering, East China University of Science and Technology, Shanghai 200237, PR China

*Corresponding to: Wei Wu. Tel./Fax: 021-64250850. E-mail: wuwei@ecust.edu.cn.

Abstract

The deoxybenzoined-based copolyarylate of BHDB-IPC with perfect charring ability was synthesized. The synergistic effects of BHDB-IPC as a charring agent in TPEE flame retarded by the phosphorous-nitrogen flame retardant (P-N FR) based on the AlPi/MCA were studied using the limiting oxygen index (LOI), the UL94 test, thermogravimetric analysis (TGA), temperature-depend FTIR, laser Raman spectroscopy (LRS), and scanning electron microscopy (SEM). The UL94 test showed that with the BHDB-IPC added to TPEE/P-N FR systems had a synergistic FR effect in condensed phase with AlPi. The TGA data illustrated that BHDB-IPC increased the thermal stability of the TPEE/P-N FR systems and especially the residues at high temperature (T＞700^{o}C). The synergistic mechanisms between AlPi and BHDB-IPC were analyzed from the temperature-depend FTIR. The residues were analyzed with LRS and SEM, which could provide useful information on the carbonaceous microstructures and the morphological structures. It was demonstrated that the BHDB-IPC promoted the information of stable and compact carbonaceous char which could prevent the melt dripping and improve the flame retardancy. Thus, BHDB-IPC was a promising synergist for the P-N flame retardant in TPEE.

Key words：thermoplastic polyether ester; flame retardant; BHDB-IPC; char formation

1. Introduction

Thermoplastic polyether ester elastomer (TPEE) consisting of hard segments (PBT chains) and soft segments (polyether chains) has the properties of rubber-flexibility, high elasticity and reversible deformation. Better yet, TPEE can be processed and modified with the thermoplastic resin processes and modification methods. Due to these excellent properties, in some areas TPEE has replaced rubbers currently with more broaden applications [1]. However, like most polymer materials, conventional TPEE composites are easy to burn with flaming droppings that may limit the application of TPEE. Traditionally, the TPEE has been mainly flame retarded by adding halogen flame retardants, such as decabromodiphenyl ethane synchronized with antimony trioxide (DBDPE/Sb_2O_3) [2, 3], but during combustion halogen flame retardants almost decompose and release dioxin which endangers the safety of humans as well as the environment [4, 5]. Thus, such halogen containing flame retardants have been banned and gradually being replaced.

Intumescent flame retardant (IFR) is fast developing as a novel kind of non-halogen flame retardant with phosphorus and nitrogen as the main effective ingredients containing acid source, gas source and carbon source at the same time. To achieve the most ideal flame retardant effect, synergistic agents can be necessary [6, 7]. Few researches have reported that phosphorous-nitrogen flame retardants with synergistic agents such as OMMT [8], novlac [9], CNTs or MoS_2 [10] can be effective on flame retarding TPEE. High efficient and stable carbon agents are of great significance to improve the efficiency of IFRs, and thus research on carbon agents is becoming a hotspot in flame retardants [11, 12]. Ranganathan [13, 14] has reported that deoxybenzoin-based copolymers can be high efficient charring agents for ketone units in deoxybenzoin are easy to dehydrate into diphenylacetylene and last form phenanthrenes polymers through cyclization. Some deoxybenzoin-based copolymers have been proved to be excellent chairing agents from the TGA test with low heat release in the cone test [15]. However, no research has reported the application of deoxybenzoin-based copolymers in thermoplastic, not to mention the TPEE.

In this research, the copolyarylate of BHDB-IPC was synthesized from 4, 4'-dihydroxy acetophenone (BHDB) and isophthaloyl chloride (IPC) by solution polymerization process. Finally the halogen-free flame retarded TPEE material which reached UL94 V-0 was successfully prepared by mixing the BHDB-IPC, phosphorus-nitrogen flame ratardant with TPEE. The fire behavior, the thermolgravimetric behavior and the structure of residue chars were studied via LOI, UL94 test, TGA , LRS and SEM.

2. Experiment

2.1 Materials

Commercial TPEE (H2040, M_w≈45,000 g/mol, T_m=190^{o}C) was purchased from Sunplas Company (China). Deoxybenzoin and pyridine hydrochloride were purchased from Sigma-Aldrich. Benzyltriethylammonium chloride and isophthaloyl chloride (IPC) were purchased from Sinopharm Chemical Reagent (China). Aluminum diethylphosphinate (AlPi, OP935) was purchased from Clariant (Germany). Melamine cyanurate (MCA) was supplied by Xusen Company (Shanghai, China). The P-N flame retardant was pre-mixed from AlPi and MCA (5:1 w/w). TPEE and MCA were dried in an oven at 90^{o}C for 5h before compounding. Others were used as received.

2.2 Synthesis of BHDB and BHDB-IPC

BHDB and BHDB-IPC were synthesized via a two-step reaction presented in Scheme 1 by using a reported procedure [13, 14]. The weight of carbon residue of BHDB-IPC at 800^{o}C can reach to 43wt% after the thermogravimetric analysis (TGA) test.

(Here Sceme.1)

2.3 Sample preparation

According to many experiments and our previous studies, the best flame retardancy for TPEE/P-N can be obtained when the mass ratio of phosphorous to nitrogen is kept at 5:1 [9]. OP935 and MCA were blended first at the mass ratio of 5:1 to get the phosphorus-nitrogen flame retardant (P-N FR). Based on many previous experiments, the total content of flame retardants in TPEE composites were kept at 18% as shown in Table 1. Based on the formulations in Table 1, TPEE was melt-mixed with the other components in a torque rheometer (RM-200A, Harbin Harpro Electrical Technology co. LTD.) at 200^{o}C for 10min. After mixing, all the samples were hot pressed under 12MPa for 5min at 205^{o}C to obtain suitable test specimens for analysis.

(Here Table.1)

2.4 Characterization

Flammability. The flammability of the samples was determined by limiting oxygen index (LOI) on an HC-2 oxygen index meter (Jiangning, China) according to ASTM D2863 (specimen size: 130mm ×6mm×3mm) and by using the vertical burning test (UL 94) on a CFZ-2 type instrument (Jiangning, China) according to ASTM D3801 (specimen size: 130mm ×13mm×1.6mm).

Thermogravimetric Analysis. The TGA was performed using a STA409 PC/PG (Netzsch, Germany) thermogravmetric analyzer with 5-8 mg samples under a N_2 flowing rate of 20 ml min^{-1} at a heating rate of 10^{o}C min^{-1} from room temperature to 700^{o}C.

Real Time FTIR Spectra. The real time FTIR spectra were recorded using a Nicolet 5700 FTIR instrument equipped with a heating device having a temperature controller. The film samples were made by melting sample powders on a KBr disc and then placed in a ventilated oven at a heating rate of 10^{o}C min^{-1} from room temperature to 400^{o}C for the dynamic measurement of FTIR in situ during the thermo-oxidative degradation.

Laser Raman Spectroscopy. The LRS measurements were carried out at room temperature with a SPEX-1403 laser Raman spectrometer, with excitation provided in backscattering geometry by a 514.5 nm argon laser line focused a micrometer spot on the sample surface.

Scanning Electronic Microscopy. The SEM was used to investigate the surface of char residues of the flame-retardant TPEE after the composites were burnt at 800^{o}C for 15 min in a muffle furnace to introduce the thermo-oxidation char during combustion.

3. Results and discussion

3.1 Effects of BHDB-IPC on LOI and UL94 values of TPEE/P-N blends

To investigate the flame retardancy of the flame-retardant TPEE samples, the LOI and vertical burning ratings (UL 94) of these samples were tested. The results are given in Table 2 for all the investigated samples.

(Here Table.2)

The neat TPEE is easy to burn in air regarding the LOI value of 17.5%. The LOI value of flame retarded TPEE with the loading of 18wt% P-N FR composed of OP935 and MCA can improve greatly and reach to 29.0%. According to the literatures and our previous studies, the results of LOI testing are mainly related to the gas-phase flame retardant [16]. Thanks to the non-flammable gas decomposing from the melamine cyanurate (MCA) [17], the LOI values of all the P-N flame retarded TPEE samples increase to about 29.0%.

However with the extra adding of BHDB-IPC which functions mainly in the condensed phase, the flame retarded samples did not show significant changes in LOI values while the results of the UL94 testing turned better. Neat TPEE was easy to burn to the clamp with serious flaming dripping in the UL94 testing. In comparison, with the loading of 18wt% P-N FR, the combustion time after flame decreased to 1.43s/5.49s, for that aluminum diethyl phosphinate and melamine cyanurate can be effective FRs for most polyester resins [18]. But without flame retardant synergistic agents especially charring agents, TPEE/18P-N FR sample dripped after the second flame application and the UL94 rating can only reach to V-2, for that the carbonaceous char was loose. After 1.5wt% BHDB-IPC was added to TPEE/16.5P-N sample, the combustion time was shortened and the carbonaceous char was enhanced to some extent but the dripping couldn’t be inhibited thoroughly. Only when the loading of BHDB-IPC was to 3wt%, the UL94 rating was enhanced to V-0 from V-2 with the combustion decreased and dripping inhibited. During combustion, BHDB-IPC acts as charring agents, which could provide compact and dense protective char at the surface to prevent the flame dripping which would be in accordance with the SEM test.

3.2 Thermogravimetric behavior

In order to better understand the thermal stability of different formulations, the thermal stability of neat TPEE and flame-retard TPEE composites were analyzed by thermo gravimetric analysis (TGA) under nitrogen at a heating rate of $10^{o}C\ min^{-1}$. The mass loss and the mass loss rate curves are presented in Fig.1 and the related data are summarized in Table 3.

(Here Fig.1 & Table.3)

As can be seen in Table 3, the mass loss of BHDB-IPC begins at $445.21^{o}C$ and the mass loss is continuous with a broad mass loss rate peak appears at about $499.57^{o}C$. It can be explained that some dehydration reactions take place as the aromatization of deoxybenzoin [19]. The residue of BHDB-IPC at the end of the TGA test is 45.46%.

The decomposition of neat TPEE starts at $401.36^{o}C$ with the highest loss rate of $2.64wt\%\ min^{-1}$ at $425.47^{o}C$. There are almost no residues at $700^{o}C$ after the TGA test for that the neat TPEE decomposed completely into gaseous molecules [9]. For Sample c, with 18wt% P-N flame retardant added into the TPEE, the temperature of 5wt% mass loss, initial degradation and the maximum mass loss were decreased by about

10^{o}C, while the loss rate was reduced and the weight of residue increased to 7.20%. The reason may be that the decomposition temperature of P-N flame retardant is lower than TPEE, but there is a catalytic role played by the aluminum diethyl phosphinate (OP935), which may accelerate the charring process during the degradation [20]. No significant changes were detected in the mass loss temperature comparing Sample c with Sample d and e. Our focus was on the maximum mass loss rate and especially on the residue weight. With the loading of BHDB-IPC, the maximum loss rate decreased for that BHDB-IPC may play a role as charring agents to promote the formation of carbon layers as well as enhanced the carbon layers as mentioned in the UL94 testing. The carbon layers can slow down the degradation to a certain extent. At 700^{o}C, the residues amount of TPEE/16.5P-N/1.5BHDB-IPC and TPEE/15.0P-N/3.0BHDB-IPC was 11.80% and 16.05%, which all exceeded the calculated ones which demonstrated that BHDB-IPC could strengthen the action of the condensed phase. All of the results show that a strong interaction between the BHDB-IPC and P-N flame retardant system occurred during the thermal degradation process and thus improved the flame retardant properties of TPEE composites.

3.3 Changes of dynamic FTIR spectra with the pyrolysis temperature

Fig.4 presents the changes of dynamic FTIR spectra obtained from the thermo-oxidative degradation of the BHDB-IPC, TPEE/18P-N and TPEE/18P-N/3.0BHDB-IPC samples, respectively, in the condensed phase with increasing pyrolysis temperature. The flame retardant mechanism of AlPi in TPEE has been studied and shown in the references [9]. Here more attention was focused on the synergistic effects between BHDB-IPC and AlPi.

The most interesting region in Fig.2 is located at 1600-1700 cm^{-1}. The peak in Fig.2a and Fig.2c at about 1660 cm^{-1} has been assigned to the various -C=O- thermo-oxidation products, which can be linked to the thermo-oxidative degradation of the BHDB-IPC.

(Here Fig.2)

For the pure BHDB-IPC, the peak at 1660 cm^{-1} shows no significant changes until 390^{o}C. But for the TPEE/18P-N/3.0BHDB-IPC blends, the decrease of the peak at 1660 cm^{-1} begins at 350^{o}C, while compared with Fig.2b peaks at 1150 cm^{-1} increase which can be assigned to the stretching mode of P-O-C in the intermediates. Based on these changes, the principle decomposition pathways for BHDB-IPC are illustrated in Fig.3.

(Here Fig.3)

As can be seen in Fig.3, with the nucleophilic reaction between the diethylphophinic acid decomposing from the AlPi and the carbonyls in the BHDB-IPC, the dehydration reaction of BHDB-IPC was accelerated and then the carbon layers formed faster at lower temperature. For the sooner and faster the formation of carbon layers is, the weight loss will be reduced in some extent which corresponded to the TGA results. In general, the synergistic effects can be attributed to the catalytic effects of the AlPi to the BHDB-IPC.

3.5 Microstructure characterization of carbonaceous charred layers

Raman scattering is especially sensitive to the structural disorder of graphite. In this work [21, 22], Raman spectroscopy was used to characterize the different types of carbonaceous structure formed in the intumescent char. Fig.4 presents the laser Raman spectra of the three samples after burnt in a muffle furnace at 800^{o}C for 15min. It can be seen that the three have a common feacture of two distinct broad peaks centered at 1580 cm^{-1} (G peak) and 1340 cm^{-1} (D peak) which have been assigned to the oriented and the disordered graphite structures [23]. And the relative intensity ratio (I_D/I_G) of the D peak to the G peak is inversely proportional to the degree of graphitization of the residual chars [24]. That is to say, the lower the I_D/I_G is, the better the structure of the chars is.

(Here Fig.4)

According to Fig.4, the incorporation of 1.5wt% BHDB-IPC into TPEE/16.5P-N decreases the I_D/I_G ratio from 2.47 to 2.25 which suggests an increase in the graphitization degree in the residual char. Furthermore, as the addition of BHDB-IPC reaches 3.0wt%, the I_D/I_G ratio decreases from 2.25 to 2.02 which showed the highest graphitization degree and the most thermally stable char structure was found in the sample of TPEE/15.0P-N/3.0BHDB-IPC. The results of the laser Raman spectra indicated that the BHDB-IPC additives could promote the formation of more compact char layers which is in good agreement with the mentioned TGA and UL94 results.

3.6 Morphological structures of residual chars

All the samples were burnt in a muffle furnace at 800^{o}C for 15min. The neat TPEE burnt out without any residues left after the furnace-burning test. The digital photographs and the SEM images of residues for Formulation 2-4 are shown in Fig.5 and Fig.6.

(Here Fig.5)

As can be seen in Fig.5, the digital photographs demonstrate that the neat TPEE almost burns out without any residues left, however there is much residual char for flame-retardant TPEE composites. The char of 18P-N flame-retardant TPEE (Fig.5(2)) is not integrated, while the char of flame-retardant TPEE with BHDB-IPC is compact and strong especially for Fig.5(4) which could be very effective in reducing mass loss as mentioned in the TGA and inhibiting drippings as mentioned in the UL94 test. It means that the incorporation of BHDB-IPC with P-N FR could improve the char residue structures and during the combustion, high effectively protective shields could be formed on the surface of char residues.

To further investigate the mechanism of BHDB-IPC on the char formation of flame-retardant TPEE during combustion, the morphologies of the char residues after the furnace-burning test were observed via SEM.

(Here Fig.6)

As can be seen in Fig.6, flame-retardant TPEE composite with 18wt% P-N FR is covered with discontinuous charred layer with many big cavities mainly due to the gas released from the gas phase flame retardant MCA [17]. With the addition of 1.5wt% BHDB-IPC, the cavities turned to be smaller, but the char surface wasn't so strong to prevent the penetration of gases that fewer flaws still exist on the surface. However, the char surface of TPEE/15.0P-N/3.0BHDB-IPC is compact, smooth and tight without any flaws. Based on these results, it is easy to understand the results from the UL94 test and the TGA test.

4. Conclusions

1. In this study, the deoxybenzoin-based polyarylate BHDB-IPC was synthesized. In the TGA test, the residues at 700 ^{o}C can reach to 45wt%.

2. A small amount of BHDB-IPC added into the phosphorous-nitrogen flame-retarded TPEE can play an important role in the UL94 test and render a V-0 classification for the TPEE/15.0P-N/3.0BHDB-IPC sample.

3. The TGA and DTG data show the addition of BHDB-IPC to the TPEE/P-N blends can improve the thermal stability. Particularly, the weight of the solid residue increased several times more than that of neat TPEE.

4. The temperature-depend FTIR shows that the AlPi can catalyze the dehydration of BHDB-IPC and accelerate the formation of carbon layers.

5. The residue analyses via LRS and SEM provide positive evidence that the TPEE/P-N blends with BHDB-IPC can form more compact microstructures in charred

layers and thus enhance the flame retardancy in the condensed phase.

Reference

[1] Amin S, Amin M, *Rev. Adv. Mater. Sci*, 2011, **29**, 15.

[2] Ziyun T, Ping H, Xianjiang X, et al. *China Elastomerics*, 2013, **4**, 002.

[3] Xi X, Qunzhao Z, Hui Z, et al. *Engineering Plastics Application,* 2013, **5**, 022.

[4] Wyrzykowska-Ceradini B, Gullett B K, Tabor D, et al, *Environmental science & technology,* 2011, **45**(13), 5853.

[5] Sakai S, Watanabe J, Honda Y, et al, *Chemosphere*, 2001, **42**(5), 519.

[6] Chen X S, Yu Z Z, Liu W, et al. *Polymer Degradation and Stability*, 2009, **94**(9), 1520.

[7] Nie S, Hu Y, Song L, et al. *Polymers for Advanced Technologies*, 2008, **19**(8), 1077.

[8] Zhong Y, Wu W, Lin X, et al, *Journal of Applied Polymer Science*, 2014, **131**(22).

[9] Zhong Y, Wu W, Wu R, et al, *Polymer Degradation and Stability*, 2014, **105**, 166.

[10] Zhong Y, Li M, Zhang L, et al. *Thermochimica Acta*, 2015, **613**, 87.

[11] Rongqi C, *Dyeing & Finishing*, 2011, **10**, 015.

[12] Jiang A, Cheng B, Ren Y, et al, *International Journal of Chemistry*, 2009, **1**(1), 31.

[13] Ranganathan T, Zilberman J, Farris R J, et al, *Macromolecules*, 2006, **39**(18), 5974.

[14] Ranganathan T, Ku B C, Zilberman J, et al, *Journal of Polymer Science Part A: Polymer Chemistry*, 2007, **45**(20), 4573.

[15] Ryu B Y, Moon S, Kosif I, et al, *Polymer*, 2009, **50**(3), 767.

[16] Laoutid F, Bonnaud L, Alexandre M, et al, *Materials science and engineering: R: Reports*, 2009, **63**(3), 100.

[17] Tang S, Qian L, Qiu Y, et al, *Journal of Applied Polymer Science*, 2014, **131**(15).

[18] Levchik S V, Weil E D, *Journal of Fire Sciences*, 2006, **24**(5), 345.

[19] Ranganathan T, Beaulieu M, Zilberman J, et al, *Polymer Degradation and Stability*, 2008, **93**(6), 1059.

[20] Samyn F, Bourbigot S, *P{Ranganathan, 2010 #195}olymer Degradation and Stability*, 2012, **97**(11), 2217.

[21] Pimenta M A, Dresselhaus G, Dresselhaus M S, et al, *Physical chemistry chemical physics*, 2007, **9**(11), 1276.

[22] Chieu T C, Dresselhaus M S, Endo M, *Physical Review B*, 1982, **26**(10), 5867.

[23] Sadezky A, Muckenhuber H, Grothe H, et al, *Carbon*, 2005, **43**(8), 1731.

[24] Vázquez-Santos M B, Geissler E, László K, et al, *The Journal of Physical Chemistry C*, 2011, **116**(1), 257.

Table.1 Composition of Formulations (wt%)

Formulation	**TPEE**	**P-N**	**BHDB-IPC**
1	100	0	0
2	82.0	18.0	0
3	82.0	16.5	1.5
4	82.0	15.0	3.0

Table.2 Results of LOI and UL94 Testing for Investigated Samples

NO	**Sample**	**LOI(%)**	**UL94,1.6mm bar**		
			t_1/t_2[a](s)	**Dripping**	**Rating**
1	TPEE	17.5±0.5	BC[b]	Yes/-	NR[c]
2	TPEE/18P-N	29.0±0.5	1.43/5.49	No/Yes[d]	V-2
3	TPEE/16.5P-N/1.5BHDB-IPC	28.9±0.5	1.40/3.60	No/Yes	V-2
4	TPEE/15.0P-N/3.0BHDB-IPC	28.2±0.5	1.34/2.25	No/No	V-0

[a] t1 and t2, average combustion time after the first and second applications of flame; [b] BC, burns to clamp; [c] NR, not rated; [d] No/Yes corresponds to the first/second flame application.

Table.3 Results of thermo gravimetric analysis

	Sample	**T_5% (^{o}C)**	**Tonset (^{o}C)**	**Tmax (^{o}C)**	**dw/dt(max) (wt%min^{-1})**	**Residue(wt%)**	
						Experiment	**Theory**
a	BHDB-IPC	395.55	445.21	499.57	-0.425	45.56	-
b	TPEE	390.83	401.36	425.47	-2.64	1.67	-
c	TPEE/18P-N	376.62	389.47	415.74	-2.08	7.20	-
d	TPEE/16.5P-N/1.5BHDB-IPC	374.31	388.52	414.62	-2.02	11.80	7.78
e	TPEE/15.0P-N/3.0BHDB-IPC	370.44	387.75	410.96	-1.84	16.05	8.35

Note: T_5% is the temperature of 5wt% mass loss; Toneset is the temperature of 10wt% loss; Tmax is the temperature of the maximum mass loss; dw/dt(max) is the maximum mass loss rate; Residue is the weight of the residue at 700^{o}C after TGA test.

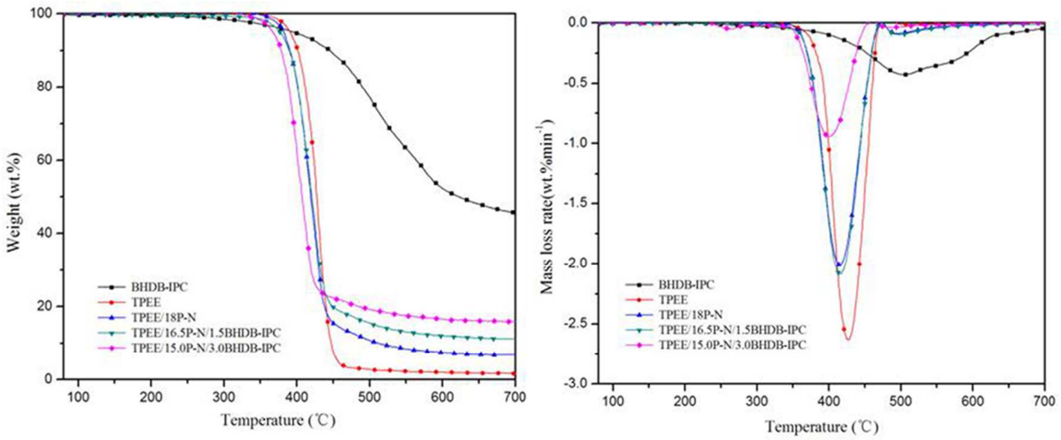

Fig.1 Mass and mass loss rate curves of all samples under nitrogen atmosphere, heating rate 10 ℃ min

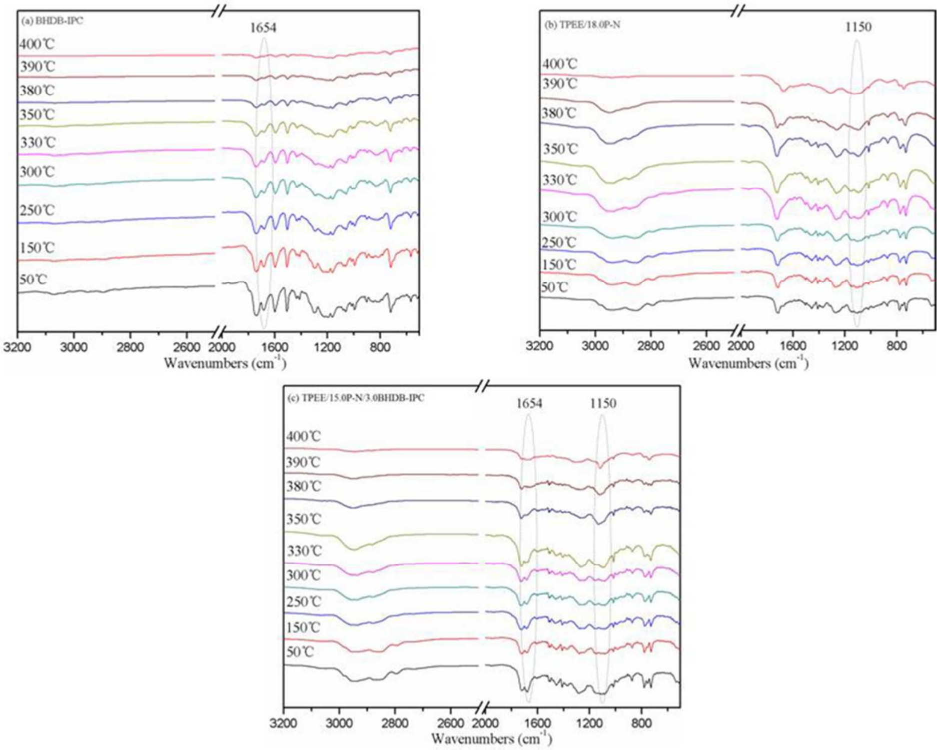

Fig.2 Dynamic FTIR spectra at different pyrolysis temperature (a) BHDB-IPC; (b) TPEE18P-N; (c) TPEE15P-N3

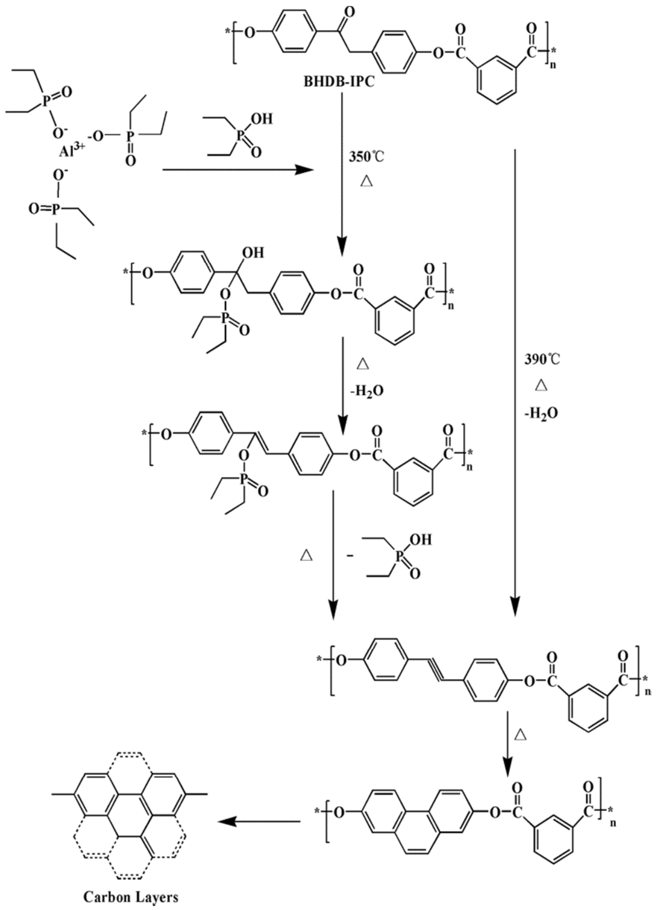

Fig.3 Main decomposition mode of BHDB-IPC

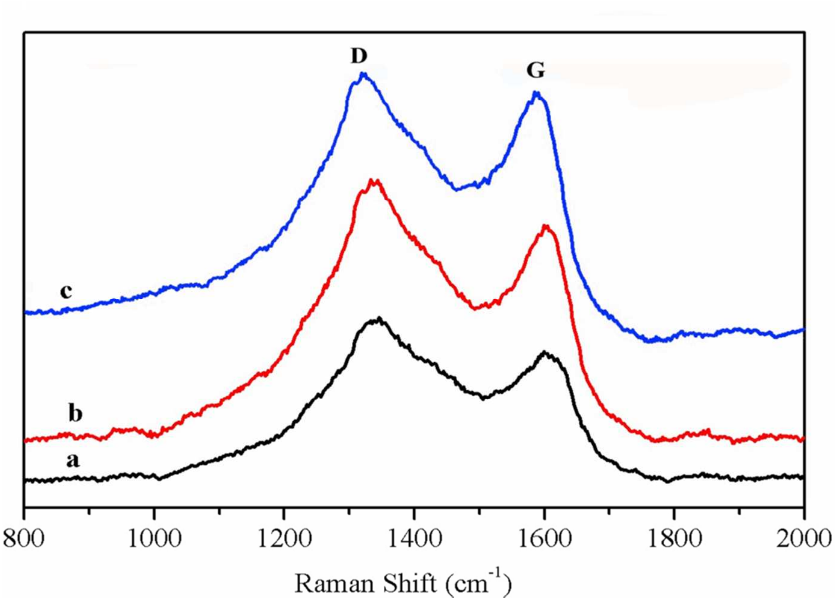

Fig.4 Laser Raman spectra of the intumescent char residues obtained from the samples after burnt in a muffle furnace at 800 ℃ for 15min

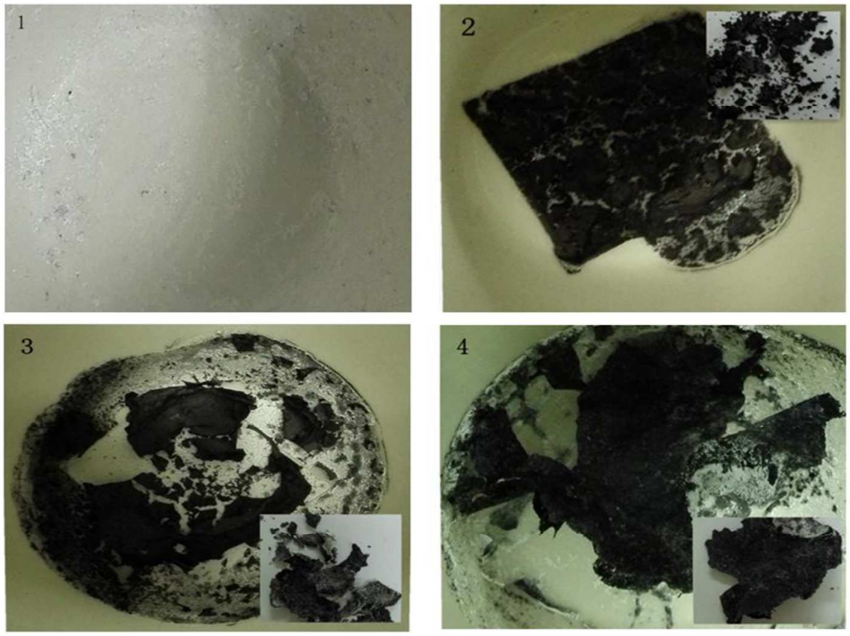

Fig.5 The digital photographs of the charred residue for Formulation 1-4

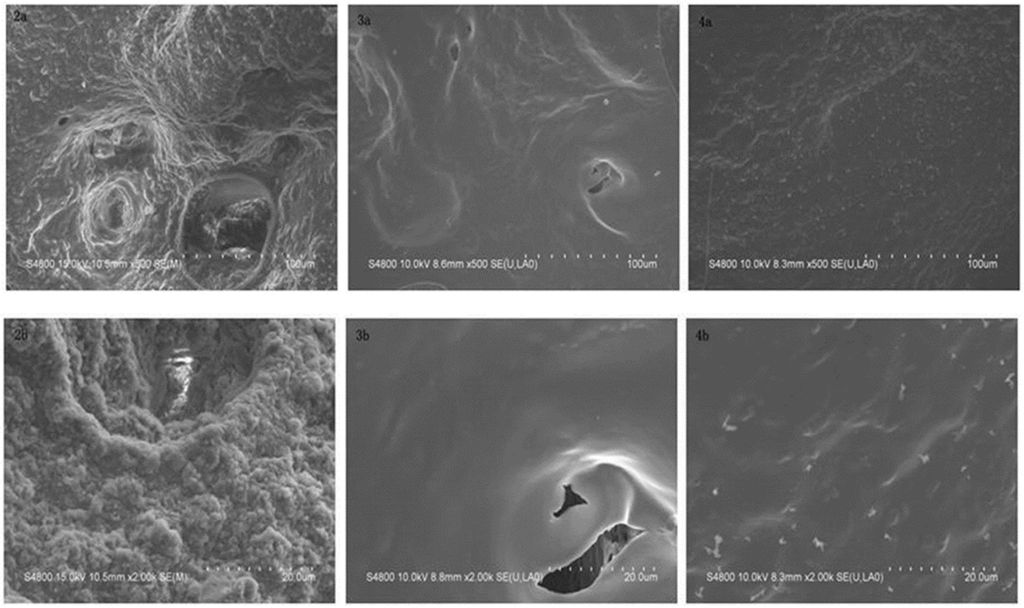

Fig.6 SEM images of the charred residue for Formulation 2, 3 and 4 at (a) low (500×) a

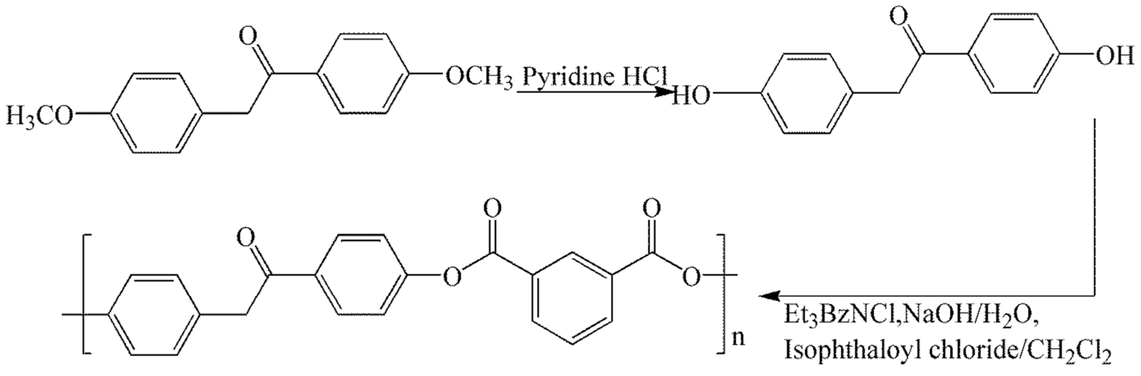

Scheme 1. Scheme of synthesis of BHDB and BHDB-IPC